Article

Widespread deoxygenation of temperate lakes

https://doi.org/10.1038/s41586-021-03550-y

Received: 28 June 2019

Accepted: 13 April 2021

Published online: 2 June 2021

Check for updates

Stephen F. Jane[1,2], Gretchen J. A. Hansen[3], Benjamin M. Kraemer[4], Peter R. Leavitt[5,6], Joshua L. Mincer[1], Rebecca L. North[7], Rachel M. Pilla[8], Jonathan T. Stetler[1], Craig E. Williamson[8], R. Iestyn Woolway[9,10], Lauri Arvola[11], Sudeep Chandra[12], Curtis L. DeGasperi[13], Laura Diemer[14], Julita Dunalska[15,16], Oxana Erina[17], Giovanna Flaim[18], Hans-Peter Grossart[19,20], K. David Hambright[21], Catherine Hein[22], Josef Hejzlar[23], Lorraine L. Janus[24], Jean-Philippe Jenny[25], John R. Jones[7], Lesley B. Knoll[26], Barbara Leoni[27], Eleanor Mackay[28], Shin-Ichiro S. Matsuzaki[29], Chris McBride[30], Dörthe C. Müller-Navarra[31], Andrew M. Paterson[32], Don Pierson[2], Michela Rogora[33], James A. Rusak[32], Steven Sadro[34], Emilie Saulnier-Talbot[35], Martin Schmid[36], Ruben Sommaruga[37], Wim Thiery[38,39], Piet Verburg[40], Kathleen C. Weathers[41], Gesa A. Weyhenmeyer[2], Kiyoko Yokota[42] & Kevin C. Rose[1]✉

The concentration of dissolved oxygen in aquatic systems helps to regulate biodiversity[1,2], nutrient biogeochemistry[3], greenhouse gas emissions[4], and the quality of drinking water[5]. The long-term declines in dissolved oxygen concentrations in coastal and ocean waters have been linked to climate warming and human activity[6,7], but little is known about the changes in dissolved oxygen concentrations in lakes. Although the solubility of dissolved oxygen decreases with increasing water temperatures, long-term lake trajectories are difficult to predict. Oxygen losses in warming lakes may be amplified by enhanced decomposition and stronger thermal stratification[8,9] or oxygen may increase as a result of enhanced primary production[10]. Here we analyse a combined total of 45,148 dissolved oxygen and temperature profiles and calculate trends for 393 temperate lakes that span 1941 to 2017. We find that a decline in dissolved oxygen is widespread in surface and deep-water habitats. The decline in surface waters is primarily associated with reduced solubility under warmer water temperatures, although dissolved oxygen in surface waters increased in a subset of highly productive warming lakes, probably owing to increasing production of phytoplankton. By contrast, the decline in deep waters is associated with stronger thermal stratification and loss of water clarity, but not with changes in gas solubility. Our results suggest that climate change and declining water clarity have altered the physical and chemical environment of lakes. Declines in dissolved oxygen in freshwater are 2.75 to 9.3 times greater than observed in the world's oceans[6,7] and could threaten essential lake ecosystem services[2,3,5,11].

The concentration of dissolved oxygen (DO) in aquatic systems influences biodiversity[1,2], nutrient biogeochemistry[3], greenhouse gas emissions[4], the quality of drinking water[5], and, ultimately, human health[12]. Many aquatic species require well-oxygenated habitats[11,13] and cool water to survive warm summers[2,11]. Loss of deep-water DO degrades water quality by promoting the release of accumulated nutrients from sediments into water[1,3], which can increase phytoplankton biomass. This process can also facilitate harmful algal blooms[5], which can compromise water supplies and harm human health[12]. Despite clear evidence of large-scale deoxygenation in ocean waters[6,7], there are no systematic large-scale studies of this phenomenon in lakes[3].

Concentrations of DO should decline with increasing water temperature owing to reduced gas solubility. However, other mechanisms can also alter DO, potentially amplifying or counteracting losses predicted from solubility changes alone. For example, the rates of heterotrophic respiration increase with temperature faster than those of primary production[9], and surface-temperature warming can increase the strength and duration of thermal stratification, reducing water circulation, and preventing deep-water DO replenishment[8,14,15]. Studies of individual lakes demonstrate that deep-water DO concentrations can decrease with lake warming[3,8,15,16], and reduce access to cold-water habitats that are essential to many organisms[11]. However, given the many feedbacks and processes regulating DO, overall trajectories currently defy a priori prediction.

We addressed this crucial issue by compiling and analysing an extensive database of lake temperature and DO profiles to characterize widespread and long-term changes in DO concentration and its causes. We used data from 393 temperate lake and reservoir basins,

A list of affiliations appears at the end of the paper.

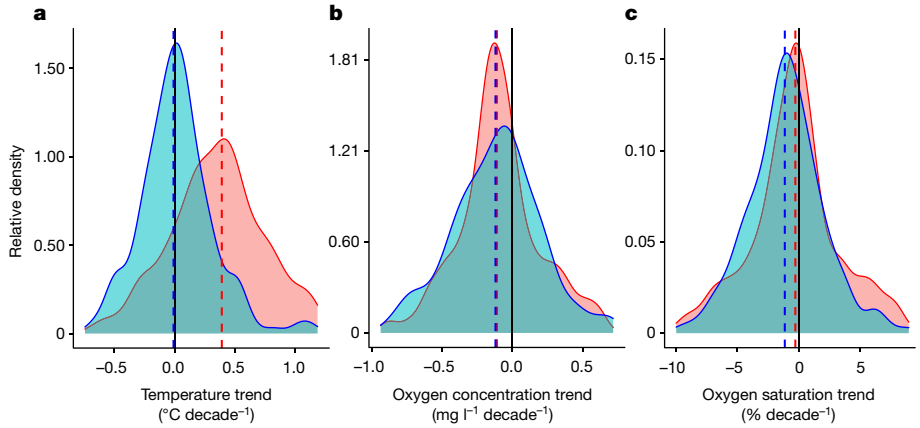

Fig. 1 | Trends in dissolved oxygen and temperature. a–c, Density plots of trend magnitudes for temperature (°C decade^{-1}) (**a**), DO concentration (mg l^{-1} decade^{-1}) (**b**) and DO percentage saturation (% decade^{-1}) (**c**). The red distribution indicates surface-water trends (n = 393), and blue indicates deep-water trends (n = 191). The x-axis range for each plot covers two standard deviations from the median, or approximately 95% of data. The vertical dashed lines indicate median trends, and the zero trend is highlighted by a black vertical line.

each with a minimum of 15 years of observation (median of 24 years) (Extended Data Fig. 1), and report population medians from long-term surface-water (epilimnion) and deep-water (hypolimnion) trends in temperature, DO concentration, and DO saturation during the late summer period when seasonal DO depletion is expected to be pronounced[17]. Our analyses showed that lake DO concentrations have declined in both surface waters and deep waters from 1980 to 2017 by 0.45 and 0.42 mg l^{-1}, respectively. These rates represent losses of 5.5% and 18.6% for surface and deep waters, respectively, and were substantially greater than those observed for the oceans, where total water-column DO has declined about 2% since 1960[6].

Although deep-water temperatures have been almost stable since observations began (−0.01 °C decade^{-1}) (Fig. 1a), both deep-water DO concentration and the percentage saturation declined over time (−0.12 mg l^{-1} decade^{-1} and −1.2% decade^{-1}, respectively) (Fig. 1b, c, Extended Data Table 1). Declines were unrelated to solubility as predicted changes based on solubility (slight increase of 0.01 mg l^{-1}) were negligible compared with observed losses (median of −0.23 mg l^{-1}) based on the last five years relative to the first five years of each time series (Fig. 2b). Despite essentially unchanging solubility, declining DO indicates that deep-water habitats have become increasingly inhospitable for organisms with aerobic metabolism, including fishes. We quantified the potential effects of such declines on habitat availability by calculating trends in T_{DO3}, the minimum water-column temperature in which DO was at least 3 mg l^{-1}. This metric was developed to quantify oxy-thermal habitats for cold-water fisheries[11]. In lakes where DO was below 3 mg l^{-1} anywhere in the water column at least once in the time series (n = 369), T_{DO3} increased by 0.17 °C decade^{-1}, with 68.0% of lakes having positive trends and declining habitats for many cold-water species.

In contrast to trends observed for deep waters, variation in surface-water DO concentrations was well explained by changes in gas solubility. Consistent with other global-scale lake studies[18], median air temperatures warmed at 0.30 °C decade^{-1} and median lake surface waters warmed at 0.39 °C decade^{-1}. In addition, median wind speed and precipitation declined (trends of −0.04 m s^{-1} decade^{-1} and −4.23 mm decade^{-1}, respectively), whereas shortwave radiation increased (1.88 W m^{-2} decade^{-1}) (Extended Data Table 2). Increases in surface-water temperature were best explained by increases in the spring and summer air temperature and by declines in the summer wind speed (Extended Data Table 3). The concentrations of surface-water DO declined at −0.11 mg l^{-1} decade^{-1} (Fig. 1b). Comparing the past five years relative to the first five years of each time series showed that the median change predicted owing to solubility loss was approximately 63% of the median observed decline in DO concentration, with a solubility-predicted loss of 0.12 versus observed losses of 0.19 mg l^{-1} (Fig. 2a).

Despite a strong influence of water temperature on DO concentration in surface waters, there was substantial variability among lakes (Fig. 2a), and a large subset of lakes exhibited increases in both water temperature and DO concentration (n = 87) (Fig. 3d). Analysis of the interaction between DO concentration, surface temperature, and water clarity (measured as Secchi depth, a proxy for trophic status[19]) showed that the DO concentration generally decreased with increasing temperature. However, in lakes with low water clarity (Secchi depth < 2 m), DO concentration increased when average mean summer surface-water temperatures exceeded around 24 °C (Fig. 3c). Similarly, in a subset of lakes with chlorophyll data (a proxy for phytoplankton biomass; n = 166), positive DO trends were observed when chlorophyll was high and surface temperatures exceeded around 25 °C, (Fig. 3b; P < 0.001). Thus, we suggest that eutrophication and warming interact to increase surface-water DO concentration despite reduced gas solubility.

Lakes with increasing DO concentration in warming surface waters had significantly higher surface-water temperatures (Fig. 3a; P = 0.016) and their watersheds contained a significantly higher proportion of agriculture (P = 0.046) and developed land cover (P = 0.001) compared with other lakes. When developed land exceeded approximately 50% of a watershed and surface water temperature exceeded 25 °C, the probability of a warming lake having an increasing DO trend was about 31%. Combined, these analyses highlight a potential threshold above which water temperatures and lake productivity interact to increase DO concentration in surface waters despite declining gas solubility. Although we lack data on the taxonomic composition of phytoplankton, evidence indicates that phytoplankton blooms are increasing globally[20], in particular owing to cyanobacteria[21]. High temperatures and increased nutrient loading can promote surface cyanobacteria blooms whose photosynthesis leads to DO supersaturation, particularly in eutrophic lakes as temperatures exceed 23–25 °C[10,21]. Consistent with this inferred mechanism, we note that these same lakes exhibited consistently low concentrations of deep-water DO (median: 0.64 mg l^{-1}) relative to other lakes (median of 3.42 mg l^{-1}), as is expected when a large phytoplankton biomass sinks and is decomposed in deep-water habitats[22]. Deep water DO changes are described in more detail below.

Decadal-scale trends in DO were associated with nonlinear changes in surface-water temperature (Fig. 2c–f, Extended Data Fig. 2). For example, although surface-water temperatures generally increased

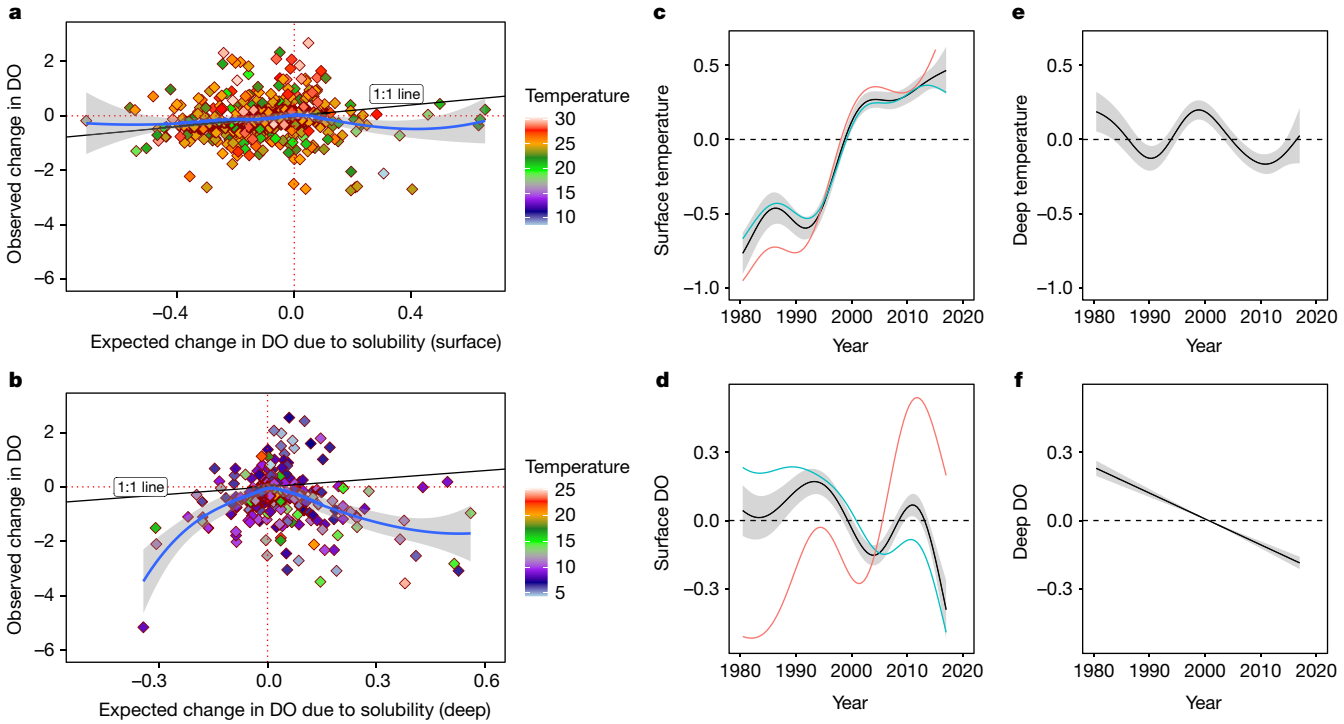

Fig. 2 | Solubility effects and changes in temperature and DO concentration over time. a, **b**, Observed versus predicted change in DO concentration (mg l^{-1}) owing to solubility for surface (**a**; $n = 415$) and deep (**b**; $n = 259$) waters. The solid black line is the 1:1 line, and the blue line is loess smoothed. Grey regions denote 95% confidence intervals. **c**–**f**, Smoothed curves of GAMM models, showing deviation from the mean model predictions for selected response variables with year as the predictor variable. Grey regions represent one standard error from the predicted line for temperature (°C) (**c**) and DO (mg l^{-1}) (**d**) over time for surface waters. The red line represents lakes in which both surface temperature and DO were increasing ($n = 87$), and the blue line denotes all other lakes ($n = 332$). **e**, **f**, Temperature (**e**) and DO (**f**) for deep waters.

from 1980 onwards, there was a period of accelerated increase from 1990 to 2000, with slower warming thereafter (Fig. 2c), consistent with the 'warming hiatus' observed from 1998 to 2012[23]. This trend occurs across the population of all lakes, as well as the subset of lakes sampled continuously throughout this period. Similarly, surface-water DO exhibited periodic deviations from an overarching trend of declining DO concentration (Fig. 2d), mainly owing to the productive lakes exhibiting increasing DO levels in surface waters (Fig. 2d, red line). Excluding these lakes, analysis of the remaining sites showed a consistent long-term decline in surface-water DO (Fig. 2d, blue line). Deep-water temperatures exhibited a pronounced multi-decadal oscillation since 1980 (Fig. 2e), as has been observed in some lakes previously[24], whereas deep-water DO concentrations declined consistently over time (Fig. 2f).

Although changes in surface-water DO concentration were generally well predicted by solubility changes, deep-water DO changes were more strongly associated with changes in water clarity and water-column density stratification (Fig. 4). For example, water clarity losses that exceeded 1 m were associated with substantial reductions in deep-water DO saturation (Extended Data Fig. 3). Mechanistically, increases in phytoplankton biomass or dissolved organic matter reduce water clarity while increasing oxygen-consuming respiration[19,22,25]. Increases in phytoplankton biomass and dissolved organic matter are often caused by changes in land use and recovery from acid deposition, respectively[26]. However, there was no overarching decline in water clarity across study lakes. Indeed, 51% of lakes had clarity increases and 49% had decreases, and only 39% of lakes exhibited both water clarity loss and DO saturation loss (Fig. 4a).

Deep-water DO decreased substantially in lakes where the water column density difference between surface and deep waters increased by more than around 0.5 kg m^{-3} (Fig. 4b, Extended Data Fig. 3b). Strong increases in the density difference indicate intensified stratification that reduces vertical mixing and replenishment of deep-water DO from the atmosphere, and may reduce nutrient upwelling to surface waters[3,15]. Differences in water column density increase owing to water clarity losses as well as other factors that increase heat gain in near-surface waters, including climate warming[26] and atmospheric stilling[27]. Increased water column density differences may also be associated with earlier onset of seasonal stratification and thus more time for oxygen consumption before the summer sampling period[22]. We found that changes in water-column density differences were best explained by changes in deep-water temperature and climate characteristics (Extended Data Fig. 4). Despite no overarching among-lake trend in water clarity or deep-water temperature, stratification strength increased in 84% of lakes that stratified, with 61% of basins exhibiting both increased density difference and DO saturation loss (Fig. 4b). Warming surface-water temperatures combined with unchanging deep-water temperatures (Fig. 1a) increases the density difference in lake water columns (median rate: 0.10 kg m^{-3} $decade^{-1}$). We observed unchanging deep-water DO in lakes where both clarity and stratification were unchanged (Fig. 4c, d). Therefore, we anticipate further DO losses in deep waters of lakes where water clarity continues to decline or thermal stratification intensifies, whether owing to atmospheric warming, stilling, or both[26,27].

Despite a wide range of lake and catchment characteristics, the overall trend of temperate lake deoxygenation is clear, with climate changes and water clarity losses contributing to declines in lake DO concentration substantially more rapid than those observed in the global oceans[6,7]. We find deep-water lake habitats are especially threatened, and deep-water DO trends may portend future losses of cold-water and oxygen-sensitive species[2], increased internal nutrient loading which exacerbates eutrophication[3] and the formation of harmful algal blooms[5], and potentially increased storage and subsequent outgassing

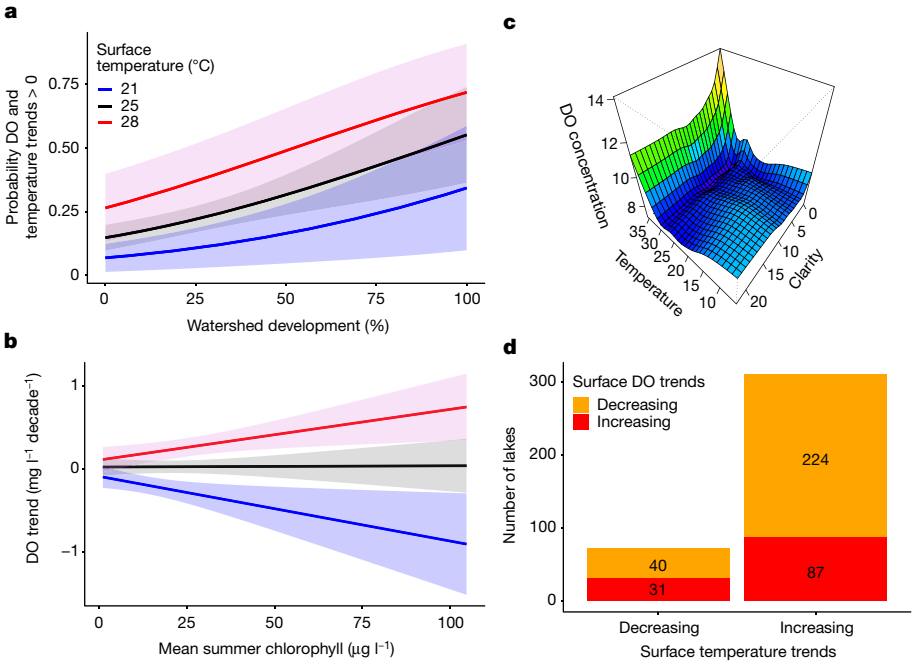

Fig. 3 | Interaction of productivity and temperature in surface waters. **a**, Predicted probability of a lake having both increasing surface temperature and DO concentration from a fitted logistic regression model at three different mean surface water temperatures: 21 °C (blue), 25 °C (black) and 28 °C (red) (n = 297). **b**, Predictions of DO trends from a fitted multiple regression model for chlorophyll (used as a surrogate for primary productivity) at these same temperatures (legend as in **a**; n = 166). **c**, The interaction of water clarity (measured as Secchi depth in metres) and surface-water temperature (°C) and their effects on surface DO (mg l^{-1}) from fitted generalized additive mixed models (GAMM). **d**, Most lakes exhibited increasing surface temperatures and decreasing DO concentration consistent with solubility effects, but a subset of lakes (n = 87) have both increasing surface temperature and DO concentration.

of methane[4]. Although already rapid, future losses in lake DO may accelerate owing to continued anthropogenic modifications of the environment, including eutrophication[22], salinization[28] and hydrological management[28]. Many lakes have undergone active management to reduce nutrient loads, in part to mitigate phytoplankton growth and deep-water oxygen loss[28], but our findings suggest such actions will probably require more rigorous efforts in the future to counter the effects of climate and land-use change.

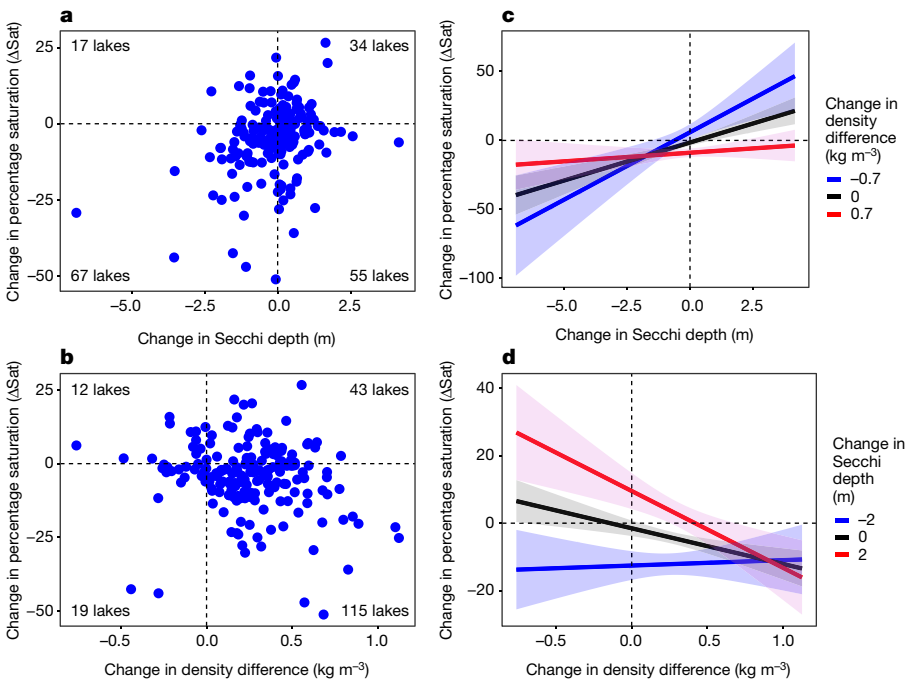

Fig. 4 | Effect of changes in water clarity and density difference on deep-water DO saturation change. **a**, Change in the percentage saturation (ΔSat) versus change in water clarity (Secchi depth). **b**, Change in the percentage saturation versus change in water column density difference between surface and deep waters. The number of lakes in each quadrant in **a** and **b** are indicated. **c**, Predictions of change in the percentage saturation from a fitted multiple regression model for change in water clarity at three density changes. **d**, Predictions of change in the percentage saturation from a fitted multiple regression model for change in density difference at three clarity changes. Note that for both **c** and **d**, the origin sits at no change in either predictor.

Online content

Any methods, additional references, Nature Research reporting summaries, source data, extended data, supplementary information, acknowledgements, peer review information; details of author contributions and competing interests; and statements of data and code availability are available at https://doi.org/10.1038/s41586-021-03550-y.

1. Wetzel, R. G. In *Limnology* 3rd edn (ed. Wetzel, R. G.), Ch. 9, 151–168 (Academic Press, 2001).
2. Schindler, D. Warmer climate squeezes aquatic predators out of their preferred habitat. *Proc. Natl Acad. Sci. USA* **114**, 9764–9765 (2017).
3. North, R. P., North, R. L., Livingstone, D. M., Köster, O. & Kipfer, R. Long-term changes in hypoxia and soluble reactive phosphorus in the hypolimnion of a large temperate lake: consequences of a climate regime shift. *Glob. Change Biol.* **20**, 811–823 (2014).
4. Fernández, J. E., Peeters, F. & Hofmann, H. Importance of the autumn overturn and anoxic conditions in the hypolimnion for the annual methane emissions from a temperate lake. *Environ. Sci. Technol.* **48**, 7297–7304 (2014).
5. Michalak, A. M. et al. Record-setting algal bloom in Lake Erie caused by agricultural and meteorological trends consistent with expected future conditions. *Proc. Natl Acad. Sci. USA* **110**, 6448–6452 (2013).
6. Schmidtko, S., Stramma, L. & Visbeck, M. Decline in global oceanic oxygen content during the past five decades. *Nature* **542**, 335–339 (2017).
7. Breitburg, D. et al. Declining oxygen in the global ocean and coastal waters. *Science* **359**, (2018).
8. Jankowski, J., Livingstone, D. M., Bührer, H., Forster, R. & Niederhauser, P. Consequences of the 2003 European heat wave for lake temperature profiles, thermal stability, and hypolimnetic oxygen depletion: implications for a warmer world. *Limnol. Oceanogr.* **51**, 815–819 (2006).
9. Yvon-Durocher, G., Jones, J. I., Trimmer, M., Woodward, G. & Montoya, J. M. Warming alters the metabolic balance of ecosystems. *Phil. Trans. R. Soc. B* **365**, 2117–2126 (2010).
10. Seki, H., Takahashi, Y., Hara, Y. & Ichimura, S. Dynamics of dissolved oxygen during algal bloom in Lake Kasumigaura, Japan. *Water Res.* **14**, 179–183 (1980).
11. Jacobson, P. C., Stefan, H. G. & Pereira, D. L. Coldwater fish oxythermal habitat in Minnesota lakes: influence of total phosphorus, July air temperature, and relative depth. *Can. J. Fish. Aquat. Sci.* **67**, 2002–2013 (2010).
12. Harke, M. J. et al. A review of the global ecology, genomics, and biogeography of the toxic cyanobacterium, *Microcystis* spp. *Harmful Algae* **54**, 4–20 (2016).
13. Vaquer-Sunyer, R. & Duarte, C. M. Thresholds of hypoxia for marine biodiversity. *Proc. Natl Acad. Sci. USA* **105**, 15452–15457 (2008).
14. Woolway, R. I. & Merchant, C. J. Worldwide alteration of lake mixing regimes in response to climate change. *Nat. Geosci.* **12**, 271–276 (2019).
15. Livingstone, D. M. Impact of secular climate change on the thermal structure of a large temperate central European lake. *Clim. Change* **57**, 205–225 (2003).
16. Zhang, Y. et al. Dissolved oxygen stratification and response to thermal structure and long-term climate change in a large and deep subtropical reservoir (Lake Qiandaohu, China). *Water Res.* **75**, 249–258 (2015).
17. Bouffard, D., Ackerman, J. D. & Boegman, L. Factors affecting the development and dynamics of hypoxia in a large shallow stratified lake: hourly to seasonal patterns. *Wat. Resour. Res.* **49**, 2380–2394 (2013).
18. O'Reilly, C. M. et al. Rapid and highly variable warming of lake surface waters around the globe. *Geophys. Res. Lett.* **42**, 10773–10781 (2015).
19. Nürnberg, G. K. Trophic state of clear and colored, soft- and hardwater lakes with special consideration of nutrients, anoxia, phytoplankton and fish. *Lake Reserv. Manage.* **12**, 432–447 (1996).
20. Ho, J. C., Michalak, A. M. & Pahlevan, N. Widespread global increase in intense lake phytoplankton blooms since the 1980s. *Nature* **574**, 667–670 (2019).
21. Kosten, S. et al. Warmer climates boost cyanobacterial dominance in shallow lakes. *Glob. Change Biol.* **18**, 118–126 (2012).
22. Müller, B., Bryant, L. D., Matzinger, A. & Wüest, A. Hypolimnetic oxygen depletion in eutrophic lakes. *Environ. Sci. Technol.* **46**, 9964–9971 (2012).
23. Winslow, L. A., Leach, T. A. & Rose, K. C. Global lake response to the recent warming hiatus. *Environ. Res. Lett.* **13**, 054005 (2018).
24. Livingstone, D. M. An example of the simultaneous occurrence of climate-driven "sawtooth" deep-water warming/cooling episodes in several Swiss lakes. *Verh. Int. Ver. Limnol.* **26**, 822–828 (1997).
25. Williamson, C. E. et al. Ecological consequences of long-term browning in lakes. *Sci. Rep.* **5**, (2015).
26. Rose, K. C., Winslow, L. A., Read, J. S. & Hansen, G. J. A. Climate-induced warming of lakes can be either amplified or suppressed by trends in water clarity. *Limnol. Oceanogr. Lett.* **1**, 44–53 (2016).
27. Woolway, R. I. et al. Northern hemisphere atmospheric stilling accelerates lake thermal responses to a warming world. *Geophys. Res. Lett.* **46**, 11983–11992 (2019).
28. Carpenter, S. R., Stanley, E. H. & Vander Zanden, M. J. State of the world's freshwater ecosystems: physical, chemical, and biological changes. *Annu. Rev. Environ. Resour.* **36**, 75–99 (2011).

[1]Department of Biological Sciences, Rensselaer Polytechnic Institute, Troy, NY, USA. [2]Department of Ecology and Genetics/Limnology, Uppsala University, Uppsala, Sweden. [3]Department of Fisheries, Wildlife and Conservation Biology, University of Minnesota, St Paul, MN, USA. [4]Department of Ecosystem Research, IGB Leibniz Institute for Freshwater Ecology and Inland Fisheries, Berlin, Germany. [5]Institute of Environmental Change and Society, University of Regina, Regina, Saskatchewan, Canada. [6]Institute for Global Food Security, Queen's University Belfast, Belfast, County Antrim, UK. [7]School of Natural Resources, University of Missouri, Columbia, MO, USA. [8]Department of Biology, Miami University, Oxford, OH, USA. [9]Centre for Freshwater and Environmental Studies, Dundalk Institute of Technology, Dundalk, Ireland. [10]European Space Agency Climate Office, ECSAT, Harwell Campus, Didcot, Oxfordshire, UK. [11]Lammi Biological Station, University of Helsinki, Lammi, Finland. [12]Department of Biology, Global Water Center, University of Nevada, Reno, NV, USA. [13]King County Water and Land Resources Division, Seattle, WA, USA. [14]FB Environmental Associates, Portsmouth, NH, USA. [15]Department of Water Protection Engineering and Environmental Microbiology, University of Warmia and Mazury in Olsztyn, Olsztyn, Poland. [16]Institute of Geography, University of Gdańsk, Gdańsk, Poland. [17]Department of Hydrology, Lomonosov Moscow State University, Moscow, Russia. [18]Department of Sustainable Agro-ecosystems and Bioresources, Research and Innovation Centre, Fondazione Edmund Mach, San Michele all'Adige, Italy. [19]Department of Experimental Limnology, Leibniz-Institute of Freshwater Ecology and Inland Fisheries, Stechlin, Germany. [20]Institute of Biochemistry and Biology, Potsdam University, Potsdam, Germany. [21]Plankton Ecology and Limnology Laboratory, Geographical Ecology Group, and Ecology and Evolutionary Biology, Department of Biology, The University of Oklahoma, Norman, OK, USA. [22]Wisconsin Department of Natural Resources, Madison, WI, USA. [23]Institute of Hydrobiology, Biology Centre CAS, České Budějovice, Czech Republic. [24]Bureau of Water Supply, New York City Department of Environmental Protection, Valhalla, NY, USA. [25]CARRTEL Limnology Center, Institut National de la Recherche Agronomique (INRA), Université Savoie Mont Blanc, Chambéry, France. [26]Itasca Biological Station and Laboratories, University of Minnesota, Lake Itasca, MN, USA. [27]Department of Earth and Environmental Sciences, University of Milan-Bicocca, Milan, Italy. [28]Lake Ecosystems Group, UK Centre for Ecology & Hydrology, Lancaster, UK. [29]Biodiversity Division, National Institute for Environmental Studies, Ibaraki, Japan. [30]Environmental Research Institute, Hamilton, New Zealand. [31]Department of Biology, University of Hamburg, Hamburg, Germany. [32]Ontario Ministry of the Environment, Conservation and Parks, Dorset Environmental Science Centre, Dorset, ON, Canada. [33]CNR Water Research Institute (IRSA), Verbania Pallanza, Italy. [34]Department of Environmental Science and Policy, University of California, Davis, CA, USA. [35]Departments of Biology and Geography, Université Laval, Québec, Canada. [36]Eawag, Swiss Federal Institute of Aquatic Science and Technology, Surface Waters – Research and Management, Kastanienbaum, Switzerland. [37]Department of Ecology, University of Innsbruck, Innsbruck, Austria. [38]Vrije Universiteit Brussel, Department of Hydrology and Hydraulic Engineering, Brussels, Belgium. [39]ETH Zurich, Institute for Atmospheric and Climate Science, Zurich, Switzerland. [40]National Institute of Water and Atmospheric Research Ltd (NIWA), Hillcrest, Hamilton, New Zealand. [41]Cary Institute of Ecosystem Studies, Millbrook, New York, USA. [42]Biology Department, State University of New York College at Oneonta (SUNY Oneonta), Oneonta, New York, USA. ✉e-mail: rosek4@rpi.edu

Methods

Overview

Our methods here describe how we (1) compiled and quality-checked data; (2) interpolated and delineated water layer strata; and (3) statistically analysed these data. Our statistical analyses focused on characterizing long-term trends in climate characteristics (air temperature, wind speed, precipitation, and short-wave radiation), DO concentration and saturation, water temperature, and deep-water habitat quality; identifying and characterizing potential nonlinearity in DO concentration and water temperature over time; characterizing the relationship between DO concentration changes and solubility, chlorophyll, and land use; identifying the predictors of changes in deep-water DO saturation, and characterizing meteorological drivers of surface temperature trends. These methods are described in detail in the following sections.

Data compilation and quality control

We compiled lake temperature and DO concentration water column measurements from temperate lakes (23.5° to 60° latitude north and south) collected by a wide range of government, university, and not-for-profit sources (Extended Data Fig. 1, Supplementary Table 1). To assess long-term trends in temperature and DO concentration, we required profiles be made at least once annually during the peak summertime stratification (defined as the late summer period, from 15 July to 31 August for northern hemisphere lakes, and 15 January to 28 February for southern hemisphere lakes) offshore (for example, nearest the deepest location in each lake) for at least 15 years. In some larger lakes ($n = 6$ lakes), we used profiles from two separate locations if the lake had more than one distinct basin and treated these as separate waterbodies. For some analyses other than long-term trend analyses we included lake time series data less than 15 years long, but always at least 10 years in duration (described below).

We conducted quality control on the compiled data as follows. We first removed impossible values, defined as those outside the range 0–40 for both temperature (°C) and DO concentration (mg l^{-1}). We then removed profiles from consideration if our initial quality control step process removed greater than 95% of the profile or if the profile had less than three distinct depth points. To reduce the potential effects of DO measurements made when sensors sat on or in sediments, we removed the deepest measurement for individual profiles if the maximum depth for that profile exceeded the maximum depth of 90% of the remaining profiles for a given lake.

Not all profiles surveyed the entire water column. Some lakes had some profiles in which the shallowest depth was greater than 0 (meaning near-surface measurements were not made), yet temperature measurements showed the nearest surface measurements were within the epilimnion. In these cases, we made the assumption of uniform DO and temperature from the surface to the shallowest measurement and added a 0 m depth point. We did this by either changing the minimum depth in the profile to 0 if it was less than 0.5 m, or adding a 0 depth point and assigning temperature and DO values equal to that of the minimum depth point if the minimum depth point was greater than or equal to 0.5 m but less than or equal to 3 m. If the minimum depth was greater than 3 m, we excluded the profile from analyses. If there were several values of either temperature or DO for a given depth, the mean value at this depth was used. These operations and all further analyses were conducted in R version 3.4.2[29].

In total, the above QA steps removed 2,040 profiles out of a total of 25,023 (8.2%). After processing and removing eight non-temperate lakes, we had 22,574 DO profiles with corresponding temperature profiles. There was a median of 2.1 profiles per year (range: 1–38) and 23 years of data per lake (Supplementary Table 2).

Profile interpolation and strata delineation

To generate a dataset with consistent depth resolution within and among lakes, we interpolated each temperature and DO profile from depth 0 m to the deepest depth of each profile at intervals of 0.5 m using the pchip function of the R package pracma[30]. This interpolation procedure preserves the overall shape of the profile by preventing overshooting of data values[30]. Following interpolation, we calculated temperature and stability characteristics using the R package rLakeAnalyzer[31]. We delineated the epilimnion and hypolimnion using the meta.depths function (slope = 0.1, seasonal = FALSE), which calculates the top and bottom depths of the metalimnion[31]. If the range of temperatures in the profile is less than 1 °C, the meta.depths function does not return values for the metalimnion (that is, the profile is not considered stratified).

Many lakes did not have a well-defined hypolimnion. To identify those with a hypolimnion, we first removed lakes in which the meta.depths function failed to calculate a bottom metalimnion depth for more than 10% of profiles. We then calculated the mean of the maximum profile depths across all profiles for each lake, to get a mean profile depth for the lake. If the mean value of the bottom of the metalimnion for a lake was shallower than the calculated mean profile depth for that lake, it was considered to have a hypolimnion. We defined 'surface waters' as all depths shallower than or equal to the top metalimnetic depth and 'deep waters' as all depths deeper than the bottom depth of the metalimnion.

Characterizing trends in dissolved oxygen and temperature

We calculated the mean surface-water or deep-water temperature and DO concentration and percentage saturation. For each lake, we calculated the mean surface-water or deep-water DO concentration or temperature for all profiles in a given year (in our defined late-summer period) to obtain a mean annual value. We then calculated the percentage DO saturation from temperature, DO concentration, and lake elevation data[32]. Mean annual surface-water and deep-water temperature and DO concentration measurements were then used to calculate long-term trends for surface waters ($n = 392$ lakes; median number of years per lake: 24) and deep waters ($n = 260$; median number of years: 24). All trends were calculated using the nonparametric Sen's slope in the R package openair[33]. Supplementary Table 2 contains metadata and trend information for all lakes with calculated trends. Trend data were not reported for lakes that had less than 15 years of data at a given depth, or deep-water trends in lakes that did not thermally stratify ('NA'). In one lake (T Bird, ID 118), epilimnetic water was artificially aerated and this depth layer was excluded from analysis.

For deep-water trends, lakes that were essentially anoxic (average hypolimnetic DO < 0.5 mg l^{-1}) had trend magnitudes that clustered near 0 relative to other lakes. This was not unexpected as lakes with essentially no hypolimnetic DO have little potential to lose additional DO. When calculating median trends and for graphical depiction of trends (Fig. 1), we removed these lakes ($n = 69$; difference = 191).

We conducted several analyses to examine the potential of variability in lake data over time (that is, not all lakes sampled all years of observation) or variability in space (that is, some regions sampled much more heavily than others) to influence overall population level trends (see the following sections and Extended Data Table 1).

Spatial autocorrelation and effects of lake clusters

Because the lakes included in this study were not uniformly dispersed over all continental land masses, we examined the potential of large numbers of lakes in relatively concentrated regions to drive overall patterns. To do this, we first examined spatial autocorrelation in trends in lake temperature and dissolved oxygen concentration using Moran's *I* in the R package lctools[34,35]. This statistic ranges from −1 for data that are perfectly dispersed to +1 for data that are perfectly autocorrelated. Values near zero suggest randomly distributed data. We observed weak but significant spatial autocorrelation in some variables (Moran's *I* values ranging from 0.02 to 0.27) (Extended Data Table 1).

Following this analysis, we examined the potential for the large numbers of lakes in some regions to dominate overall trends we reported. We tested for potential bias by examining trends for a subset of lakes.

We identified four regions in the US with high numbers of lakes (Maine = 113 lakes, New Hampshire = 38 lakes, Missouri = 41 lakes, and Minnesota = 84 lakes). For each of these clustered regions, we randomly subsampled 10% of the lakes. After creation of a random subset, we found that the overall trends are similar to the trends obtained from all lakes (Extended Data Table 1). These results demonstrate that our observed population-level trends are not driven solely by trends observed in our lake-rich regions. Although our analysis focuses on temperate lakes, we obtained data from a small number of non-temperate lakes (n = 8). Including these non-temperate lakes in our analysis (Extended Data Table 1) did not change our overall results.

Uncertainty estimates and temporal variation in trends

We conducted an analysis to compare trends, confidence intervals, and significance of trends over two time periods: 1980–2017 (n = 80) and 1990–2017 (n = 197) to assess whether different lake observation years influenced the overall trends in DO concentration and temperature we observed. For each time period, we used a subset of lakes that had data for at least 80% of years within the defined time period. Following established methods[18], we calculated a yearly anomaly in temperature and dissolved oxygen for each lake as the difference between each year's observation and the long-term mean. We then averaged these anomalies across all lakes and used linear regression to calculate the slope, significance, and confidence intervals of these averaged anomalies (Extended Data Table 1).

Characterizing trends in climate characteristics

We examined trends in air temperature, total precipitation, wind speed, and shortwave radiation using the ERA-5 reanalysis from the European Centre for Medium-Range Weather Forecasts (ECMWF)[36]. This data set provides a single gridded global product with a resolution of 0.25° latitude by 0.25° longitude over the period 1979–2019 available as monthly averages (air temperature, wind speed, and shortwave radiation) or totals (precipitation). We used ECMWF time-series data from the gridded location closest to each lake and over the two-month period around when lakes were sampled (July–August for Northern hemisphere lakes, January–February for Southern hemisphere lakes). We calculated temporal trends in mean summer air temperature, mean summer wind speed, summer total precipitation, mean summer shortwave radiation, mean winter air temperature, mean spring air temperature, mean autumn air temperature using the same methods we used to examine lake temperature and DO trends (see above). We then conducted a multiple regression analysis to assess which of these predictor variables (trends in air temperature, total precipitation, wind speed, or shortwave radiation) best explained surface-water temperature trends (Extended Data Table 3).

Trends in climatic variables over the temperate zone

We delineated gridded latitude and longitudes at 2° intervals across the entire temperate zone over land masses only as well as over large regions, including Asia (defined by longitude ≥ 29.3°; latitude 23.5° to 60°); Europe and North America (longitude <29.3°; latitude 23.5° to 60°); South America and western Africa (longitude <0°; latitude ≤−23.5° to −60°); and southern Africa, Australia, and Oceania (longitude ≥ 0°; latitude −23.5° to −60°). We then used data from the ERA-5 reanalysis (see 'Characterizing trends in climate characteristics' section) to calculate trends in climate variables over each of these regions (Extended Data Table 2).

Multiple regression analysis of drivers of surface water temperature trends

We conducted a multiple regression analysis of the meteorological drivers of observed surface water temperature trends. Predictors in the analysis included: summer air temperature trend, summer total precipitation trend, summer wind speed trend, summer shortwave radiation trend, winter air temperature trend, spring air temperature trend, autumn air temperature trend, and mean winter temperature (as a proxy for ice cover[18]). All variables were standardized by z-scores to facilitate comparison of model coefficients across variables having different units[37]. We verified that multicollinearity was not a problem by checking that the variance inflation factor was well below ten for all variables[38]. We used the leaps R package to select subset models including all predictors and two-way interactions, and selected the fitted model having the lowest Akaike information criterion (AIC)[39]. Coefficients and P values for the selected model appear in Extended Data Table 3.

Characterizing trends in deep-water habitat quality

We used T_{DO3}[11] to quantify trends in oxy-thermal habitat relevant for cold-water organisms. T_{DO3} represents the minimum temperature in the water column where DO concentration was greater than or equal to 3 mg l^{-1} and has been used to describe habitat availability for cold-water fisheries[11]. To calculate trends in T_{DO3} we excluded lakes where the DO concentration was higher than 3 mg l^{-1} across all depths in all profiles. For the remaining lakes, we calculated T_{DO3} for each profile. If a given profile did not have DO below 3 mg l^{-1}, we assigned it the minimum temperature in the profile. We then calculated an annual mean T_{DO3} for the late summer period and excluded lakes that had ≤15 years of data. This left 369 lakes in which DO went below 3 mg l^{-1} at least once.

Nonlinearity in DO and temperature over time

We conducted a generalized additive mixed model (GAMM) analysis to characterize overall response of lake temperature and DO concentration over time and to identify any nonlinearity. GAMMs fit a smooth function of the predictor variables showing the relationship of the predictors to the response variable[40]. We conducted separate analyses for four response variables, surface-water temperature, surface-water DO concentration, deep-water temperature, and deep-water DO concentration. For each GAMM, our only predictor variable was the year, resulting in models that show the change in the response variable over time. We used the gamm4 function of the gamm4 R package to fit these models using the default thin plate spline for smooth terms[41]. Gamm4 uses penalized regression splines of moderate rank for the smooth function. For two of these models we used a normal error distribution. Because residuals for the deep-water temperature analysis were skewed, we used a gamma distribution. Residuals in the deep-water DO analysis were also skewed, but because there were a large number of 0 values we used a Tweedie distribution instead of a gamma distribution. We limited this analysis to data from 1970 and later and included all lakes with data in the specified time period (total lake n = 417). To account for the non-independent nature of the repeated measurements over time within each individual lake, the slope and intercept were allowed to vary randomly by lake[42].

We next conducted a GAMM to understand how surface water DO concentration responded to temperature and productivity (n = 419 lakes). We used Secchi disk depth as a surrogate for productivity[19]. We included fixed effects of mean summer surface water temperature, mean Secchi depth, and the interaction of these two terms in the model. We included a random intercept and slope by year within each lake and included a corresponding year fixed effect.

Relationship between dissolved oxygen concentration changes and solubility

To determine the relative importance of solubility in explaining changes in DO concentration, we calculated the expected change in DO concentration due to solubility alone and compared this amount to the observed DO change. To do this, we first calculated the difference between the observed mean DO concentration across the last five years and the first five years of record for each lake, requiring a minimum of ten years of data per lake (n = 415 lakes for surface (Fig. 2a, Extended

Data Fig. 2); $n = 259$ lakes for deep (Fig. 2b)). We then calculated the expected change due solely to solubility and compared the observed to expected DO changes. Specifically, we calculated the mean percentage saturation in the first five years by first calculating the mean DO saturation for each water column layer (surface or deep waters), and then calculated the mean of all of these values. We then used an analogous approach to calculate mean temperature, DO concentration, and mean DO concentration at 100% saturation in the last five years of record for each lake. Once we calculated these values, we multiplied the mean DO concentration at 100% saturation by the decimal value of percentage saturation in the first five years of record. This product represents the expected DO concentration if the percentage saturation in the last five years of record remained the same as it was in the first five years of record. In other words, we removed the effect of temperature so that if all changes were due solely to solubility, observed changes in DO concentration would be identical to this value.

Relationship between dissolved oxygen trends and chlorophyll

We used multiple regression to test whether chlorophyll concentration and surface-water temperature were predictors of lakes having both increasing surface DO concentration and temperature trends. We first calculated the long-term mean late-summer surface-water (epilimnetic) chlorophyll concentration, which was available for 166 lakes having at least 10 years of chlorophyll measurements. We next predicted DO concentration trends using chlorophyll and mean surface-water temperature as independent variables. We first fit the linear regression models, starting with a full model that included the interaction of chlorophyll and temperature. We then fit all subset models and selected the model with the lowest AIC value[43]. Using this selected model, we predicted DO concentration trends at three different mean epilimnetic temperatures (21 °C, 25 °C and 28 °C) across the observed values for chlorophyll (Fig. 3b).

Relationship between dissolved oxygen trends and land use

We used logistic regression to better understand the drivers of increasing DO concentration in lakes with increasing surface-water temperatures, using land-use or land-cover data to model the probability of this phenomenon[44]. Logistic regression predicts the probability of a binary response outcome for different values of predictor variables. Predictors in our logistic regression included the percentage of agriculture and developed land cover in the watershed and the mean surface-water temperature over the last ten years of record because these land-use characteristics have been associated with increased growth of some phytoplankton taxa in warmer lakes[5,21]. Our binary response was: either a lake had both increasing surface temperature and DO concentration (1) or it did not (0). We tested for all two-way interactions and all main effects. We used the National Land Cover Database 2011 to derive land cover metrics for US lakes[45]. We considered any land falling into any of the developed classes as developed (developed–open space, developed–low intensity, developed–medium intensity, developed–high intensity). We tested the goodness of fit of the final model using the Hosmer–Lemeshow test, available in the ResourceSelection R package (function hoslem.test)[46]. This test showed an acceptable goodness of fit ($P = 0.166$). The final number of lakes for analysis that had both land-cover data and sufficient data to calculate trends was 326.

Identifying the predictors of changes in deep-water DO saturation

We first used a random forest algorithm to obtain predictors of the observed change in percentage saturation (that is, drivers beyond pure solubility effects) in deep waters[47]. We used the percentage increase in mean squared error as a measure of predictor variable importance. We conducted the random forest algorithm analysis using the randomForest R package[48]. For each analysis, we only used lakes that had no missing values for any of the predictor variables ($n = 224$ lakes).

For the random forest algorithm, the response variable was the change in mean DO percentage saturation in the past five years of record relative to the first five years of record for each lake (ΔSat). A positive ΔSat value indicated an increase in percentage saturation, whereas a negative ΔSat value indicated a decrease in percentage saturation. Predictor variables included mean hypolimnetic DO percentage saturation, DO concentration, temperature, and thickness of the hypolimnion (ln-transformed), mean Secchi depth, ln-transformed mean lake depth, $\log_{10}$-transformed residence time, change in hypolimnetic thickness, change in hypolimnetic temperature, change in Secchi depth, and change in the density difference between surface and deep waters. Mean lake depth and residence time were obtained from the HydroLakes Database[49]. We calculated the density difference across the water column using rLakeAnalyzer to calculate densities for each interpolated depth point in each water column profile[31]. If a given profile was stratified, we then used the mean epilimnetic density and the mean hypolimnetic density and calculated the difference between these densities. If a given profile was not stratified, we took the mean density across the top two meters and the mean density across the bottom two meters and calculated the difference between these densities. We also included trends in the following ERA-5 meteorological variables: summer, autumn and winter air temperature, summer shortwave radiation, and summer wind speed. Finally, we included mean winter air temperature as a proxy for ice cover[18].

Following the above analysis, change in the density difference between surface and deep waters came out as an important predictor. Although this could be explained by increased surface water temperatures driven by meteorological variables, it is possible that other changes, such as water clarity[25], could also explain changes in density difference. To disentangle the drivers of changes in water column density differences, we conducted another random forest analysis using the same predictor variables as the above analysis but changing the response variable to the change in the density difference. We did not include the response variable from the first analysis (ΔSat). The six most important variables are presented in Extended Data Fig. 4.

On the basis of the results of the random forest analysis, we conducted a multiple regression analysis to predict change in percentage saturation for different levels of predictor variables (ln-transformed mean lake depth, change in the density difference across the water column, and change in Secchi depth). We used a subset of lakes where mean deep-water DO concentration exceeded 0.5 mg l^{-1} to avoid lakes with little potential to lose DO. Predictor variables were selected because they were the three most important variables identified by random forests, except we substituted ln-transformed mean lake depth for ln-transformed deep layer thickness. This substitution was made because models using ln of deep layer thickness demonstrated substantial nonlinearity in plots of residuals against fitted values. Models built with ln mean lake depth greatly improved these patterns and these two variables were correlated ($r = 0.51$). We first fit the multiple regression models starting with a full model that included all predictors and two-way interaction terms. We then fit all subset models and selected the model with the lowest AIC value[43]. Using this selected model, we predicted ΔSat at three different values of each of the two predictors change in Secchi depth ($P < 0.001$) and change in water column density difference ($P < 0.001$), with ln mean lake depth held at the median value.

Data availability

Raw data used in this study are available in published datasets for all lakes except numbers 99, 100, 101 and 104 via the Freshwater Research and Environmental Database (number 3; https://doi.org/10.18728/568.0), the INRAE data repository (numbers 102, 127; https://doi.org/10.15454/BUJUSX), or the Environmental Data Initiative (all others; https://doi.org/10.6073/pasta/841f0472e19853b0676729221aedfb56)[50–52]. For numbers 99, 100, 101 and 104, permission was not

granted from original data providers to make raw data publicly available. Original dataset sources and contact information for all sites are described in Supplementary Table 1. Supplementary Table 2 contains reported trends in dissolved oxygen and temperature for all lakes with more than 15 years of observations.

29. R Core Team. *R: A Language and Environment for Statistical Computing*. http://www.R-project.org/ (R Foundation for Statistical Computing, Vienna, 2017).
30. Borchers, H. W. *pracma: Practical Numerical Math Functions*. R package version 2.1.5 https://CRAN.R-project.org/package=pracma (2018).
31. Winslow, L. A. et al. *rLakeAnalyzer: Lake Physics Tools*. R package version 1.11.4. https://CRAN.R-project.org/package=rLakeAnalyzer (2017).
32. Winslow, L. A. et al. LakeMetabolizer: an R package for estimating lake metabolism from free-water oxygen using diverse statistical models. *Inland Waters* **6**, 622–636 (2016).
33. Carslaw, D. C. & Ropkins, K. Openair – an R package for air quality data analysis. *Environ. Model. Softw.* **27-28**, 52–61 (2012).
34. Moran, P. A. P. The interpretation of statistical maps. *J. R. Stat. Soc. B* **10**, 243–251 (1948).
35. Kalogirou, S. *lctools: Local Correlation, Spatial Inequalities, Geographically Weighted Regression and Other Tools*. R package version 0.2-7. https://CRAN.R-project.org/package=lctools (2019).
36. Copernicus Climate Change Service (C3S). ERA5: Climate Data Store (CDS) https://cds.climate.copernicus.eu/cdsapp#!/home (accessed 1 October 2019).
37. Gelman, G. & Hill, J. *Data Analysis Using Regression and Multilevel/Hierarchical Models* (Cambridge Univ. Press, 2007).
38. Quinn, G. P. & Keough, M. J. *Experimental Design and Data Analysis for Biologists* (Cambridge Univ. Press, 2002).
39. Lumley, T. *leaps: Regression Subset Selection*. R package version 3.1. https://CRAN.R-project.org/package=leaps (2020).
40. Wood, S. N. *Generalized Additive Models: An Introduction with R* 2nd edn (CRC Press, 2017).
41. Wood, S. & Scheipl, F. *gamm4: Generalized Additive Mixed Models using 'mgcv' and 'lme4'*. R package version 0.2-5. https://CRAN.R-project.org/package=gamm4 (2017).
42. Pinheiro, J. C. & Bates, D. M. *Mixed Effects Models in S and S-Plus* (Springer, 2000).
43. Burnham, K. P., Anderson, D. R. & Huyvaert, K. P. AIC model selection and multimodel inference in behavioral ecology: some background, observations, and comparisons. *Behav. Ecol. Sociobiol.* **65**, 23–35 (2011).
44. Hosmer, D. W. & Lemeshow, S. *Applied Logistic Regression* 2nd edn (John Wiley and Sons, Inc., 2000).
45. Homer, C. G. et al. Completion of the 2011 National Land Cover Database for the conterminous United States – Representing a decade of land cover change information. *Photogramm. Eng. Remote Sensing* **81**, 345–354 (2015).
46. Lele, S. R., Keim, J. L. & Solymos, P. *ResourceSelection: Resource Selection (Probability) Functions for Use-Availability Data*. R package version 0.3-2. https://CRAN.R-project.org/package=ResourceSelection (2017).
47. Cutler, D. R. et al. Random forests for classification in ecology. *Ecology* **88**, 2783–2792 (2007).
48. Liaw, A. & Wiener, M. Classification and regression by randomForest. *R News* **2**, 18–22 (2002).
49. Messager, M. L., Lehner, B., Grill, G., Nedeva, I. & Schmitt, O. Estimating the volume and age of water stored in global lakes using a geo-statistical approach. *Nat. Commun.* **7**, 13603 (2016).
50. Stetler, J. T., Jane, S. F., Mincer, J. L., Sanders, M. N. & Rose, K. C. Long-term lake dissolved oxygen and temperature data, 1941–2018 ver 2. *Environmental Data Initiative* https://doi.org/10.6073/pasta/841f0472e19853b0676729221aedfb56 (2021).
51. Adrian, R., Jane, S. F., & Rose, K. C. Widespread deoxygenation of temperate lakes – Müggelsee data. IGB Leibniz-Institute of Freshwater Ecology and Inland Fisheries dataset. https://doi.org/10.18728/568.0 (2021).
52. Jenny, J.-P. Time series dataset of dissolved oxygen, water temperature and Secchi depths profiles in Lakes Annecy and Geneva. *Portail Data INRAE* **V1**, https://doi.org/10.15454/BUJUSX (2021).

Acknowledgements This manuscript benefited from conversations at meetings of the Global Lake Ecological Observatory Network (GLEON; supported by funding from US NSF grants 1137327 and 1702991). S.F.J. and K.C.R. acknowledge support from US NSF grants 1638704, 1754265 and 1761805, and S.F.J. was supported by a US Fulbright Student grant to Uppsala University, Sweden. G.J.A.H. acknowledges the many employees of the Minnesota Department of Natural Resources, the Minnesota Pollution Control agency, and citizen volunteers for data collection and collation. B.M.K. acknowledges the 2017-2018 Belmont Forum and BiodivERsA joint call for research proposals under the BiodivScen ERA-Net COFUND programme and with funding from the German Science Foundation (AD 91/22-1). P.R.L. acknowledges support from a NSERC Discovery Grant, the Canada Research Chair Program, Canada Foundation for Innovation, the Province of Saskatchewan, University of Regina, and Queen's University Belfast. R.L.N. and J.J. acknowledge support from the Missouri Department of Natural Resources and the Missouri Agricultural Experiment Station and many students that collected and processed reservoir samples under the leadership of Daniel V. Obrecht and Anthony P. Thorpe. R.M.P. and C.E.W. acknowledge support from NSF grants 1754276 and 1950170, Miami University Eminent Scholar Fund, and the Lacawac Sanctuary and Biological Field Station for access to Lake Lacawac and use of research facilities. R.I.W. acknowledges support from the European Union's Horizon 2020 research and innovation programme under the Marie Skłodowska-Curie grant agreement no. 791812. S.C. acknowledges support of the Castle Lake Research Program through the University of Nevada and UC Davis via Charles R. Goldman. C.L.D. acknowledges the King County Environmental Laboratory for the long-term monitoring data for Lake Washington and Lake Sammamish. J.D. acknowledges support from the University of Warmia and Mazury in Olsztyn (Grant under the Senate Committee for International Cooperation financing) and staff at Department of Water Protection Engineering and Environmental Microbiology for long-term data collection and analysis. O.E. acknowledges support from the Russian Scientific Foundation (grant 19-77-30004) for Mozhaysk Reservoir. G.F. acknowledges support for long-term sampling of Lake Caldonazzo by the Fondazione Edmund Mach. H.P.G. acknowledges funding for long-term sampling of Lake Stechlin by the Leibniz association and assistance by members of the IGB team. K.D.H. acknowledges the Oklahoma Department of Wildlife Conservation, the Oklahoma Water Resources Board, the Grand River Dam Authority, the US Army Corps of Engineers, the City of Tulsa, W. M. Matthews, T. Clyde, R. M. Zamor, P. Koenig, and R. West for support, assistance, and data for Lakes Texoma, Thunderbird, Grand, Eucha, and Spavinaw. J.H. acknowledges support from the ERDF/ESF project Biomanipulation as a tool for improving water quality of dam reservoirs (no. CZ.02.1.01/0.0/0.0/16_025/0007417) . B.L. acknowledges support from the FA-UNIMIB for long-term monitoring of Lake Iseo. E.B.M. acknowledges support from the UK Natural Environment Research Council funding for the long-term monitoring on Blelham Tarn and the staff of the Freshwater Biological Association and UK Centre for Ecology and Hydrology for carrying out the work. A.P. and J.A.R. acknowledge support from the Ontario Ministry of the Environment, Conservation and Parks for providing data from south-central Ontario lakes ('Dorset lakes') and staff and students at Ontario's Dorset Environmental Science Centre for data collection and analysis. M.R. acknowledges the International Commission for the Protection of Italian-Swiss Waters (CIPAIS) for funding long-term research on Lake Maggiore. M.S. acknowledges the City of Zurich Water Supply and the cantonal agencies of the cantons of Bern (AWA, Gewässer- und Bodenschutzlabor), Zurich (AWEL), St. Gallen (AFU), and Neuchatel for providing data for the Swiss lakes, CIPEL and INRA for data from Lake Geneva, and IGKB for data from Lake Constance. R.S. acknowledges support from the LTSER platform Tyrolean Alps (LTER-Austria).W.T. acknowledges support from the Belgian Science Policy Office through the research project EAGLES (CD/AR/02A) on Lake Kivu. P.V. acknowledges support from the councils of the regions of Waikato, West Coast, and Bay of Plenty for long-term sampling of lakes Taupo, Brunner, and Tarawera. K.Y. acknowledges support from the Clark Foundation for long-term monitoring of Otsego Lake and past and current members of SUNY Oneonta BFS for sampling. K.S. and J.S. acknowledge the National Park Service, W Gawley, Acadia National Park for providing data for Jordan Pond, Bubble Pond, and Eagle Lake in Maine. We acknowledge the support of other data contributors, including B. Adamovich, T. Zhukova and Belarusian State University; R. Adrian and the Leibniz Institute of Freshwater Ecology and Inland Fisheries; L. Bacon and the Maine Department of Environmental Protection; M. Cofrin and the New Hampshire Department of Environmental Services; S. Devlin, Flathead Lake Biological Station, and the University of Montana; E. Gaiser, H. Swain, K. Main, N. Deyrup and Archbold Biological Station; S. Higgins and the IISD Experimental Lakes Area; L. Kaminski and the Michigan Clean Water Corps and Michigan Department of Environment, Great Lakes, and Energy; Pernilla Rönnback and the Swedish University of Agricultural Sciences; S. Nierzwicki-Bauer, the Darrin Freshwater Institute, and Rensselaer Polytechnic Institute; C. Pedersen and the Minnesota Department of Natural Resources; P. Stangel and the Vermont Department of Environmental Conservation; E. Stanley and the North Temperate Lakes Long-Term Ecological Research site; and M. Vanni, M. Gonzalez and Miami University. We also acknowledge the assistance of C. Gries in making data publicly available via the Environmental Data Initiative. The views expressed in this Article are those of the authors and do not necessarily reflect views or policies of funding agencies.

Author contributions S.F.J. and K.C.R. designed the study, compiled the data, conducted analyses, and drafted the manuscript. G.J.A.H., B.M.K., P.R.L., J.L.M., R.L.N., R.M.P., J.T.S., C.E.W. and R.I.W. helped design the study and conduct analyses, contributed data, and edited the manuscript. L.A., S.C., C.L.D., L.D., J.D., O.E., G.F., H.-P.G., K.D.H., C.H., J.H., L.L.J., J.-P.J., J.R.J., L.B.K., B.L., E.M., S.-I.S.M., C.M., D.C.M.-N., A.M.P., D.P., M.R., J.A.R., S.S., E.S.-T., M.S., R.S., W.T., P.V., K.C.W., G.A.W. and K.Y. contributed data, edited the manuscript, or both.

Competing interests The authors declare no competing interests.

Additional information

Supplementary information The online version contains supplementary material available at https://doi.org/10.1038/s41586-021-03550-y.

Correspondence and requests for materials should be addressed to K.C.R.

Peer review information *Nature* thanks Peter Raymond and the other, anonymous, reviewer(s) for their contribution to the peer review of this work.

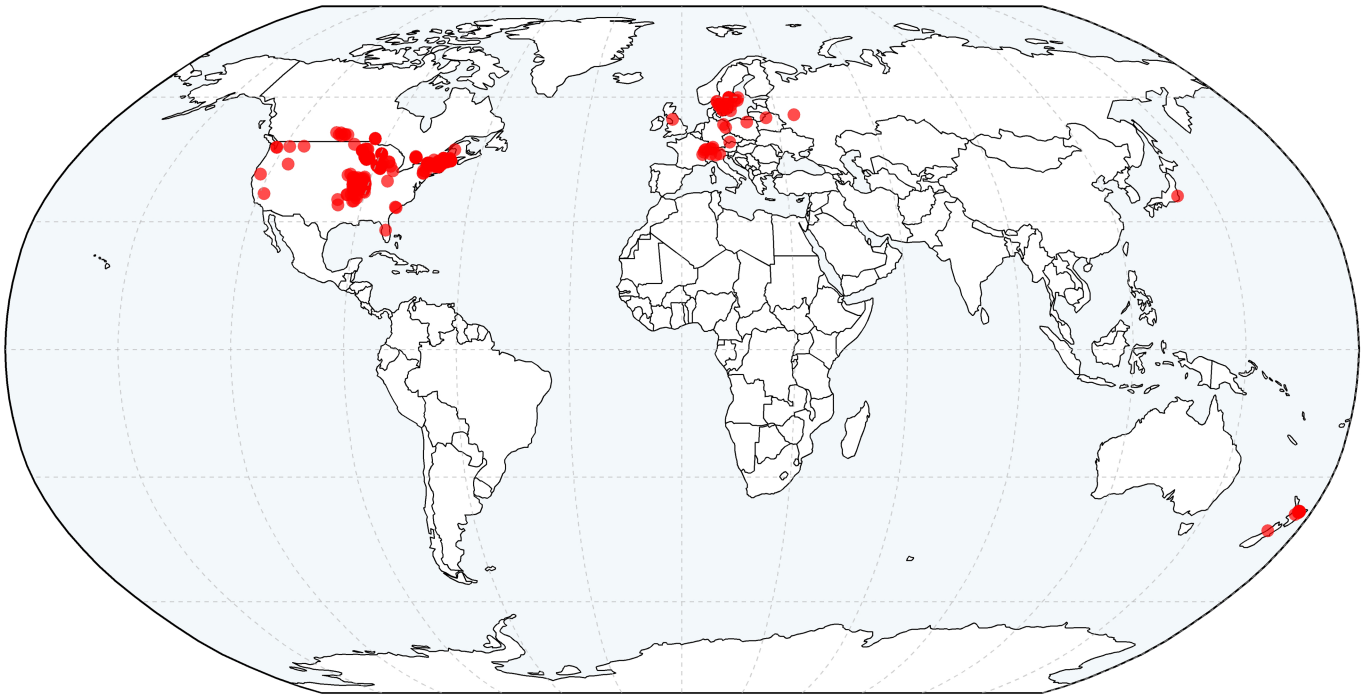

Extended Data Fig. 1 | Locations of lakes used in this study. Red circles denote the study lakes.

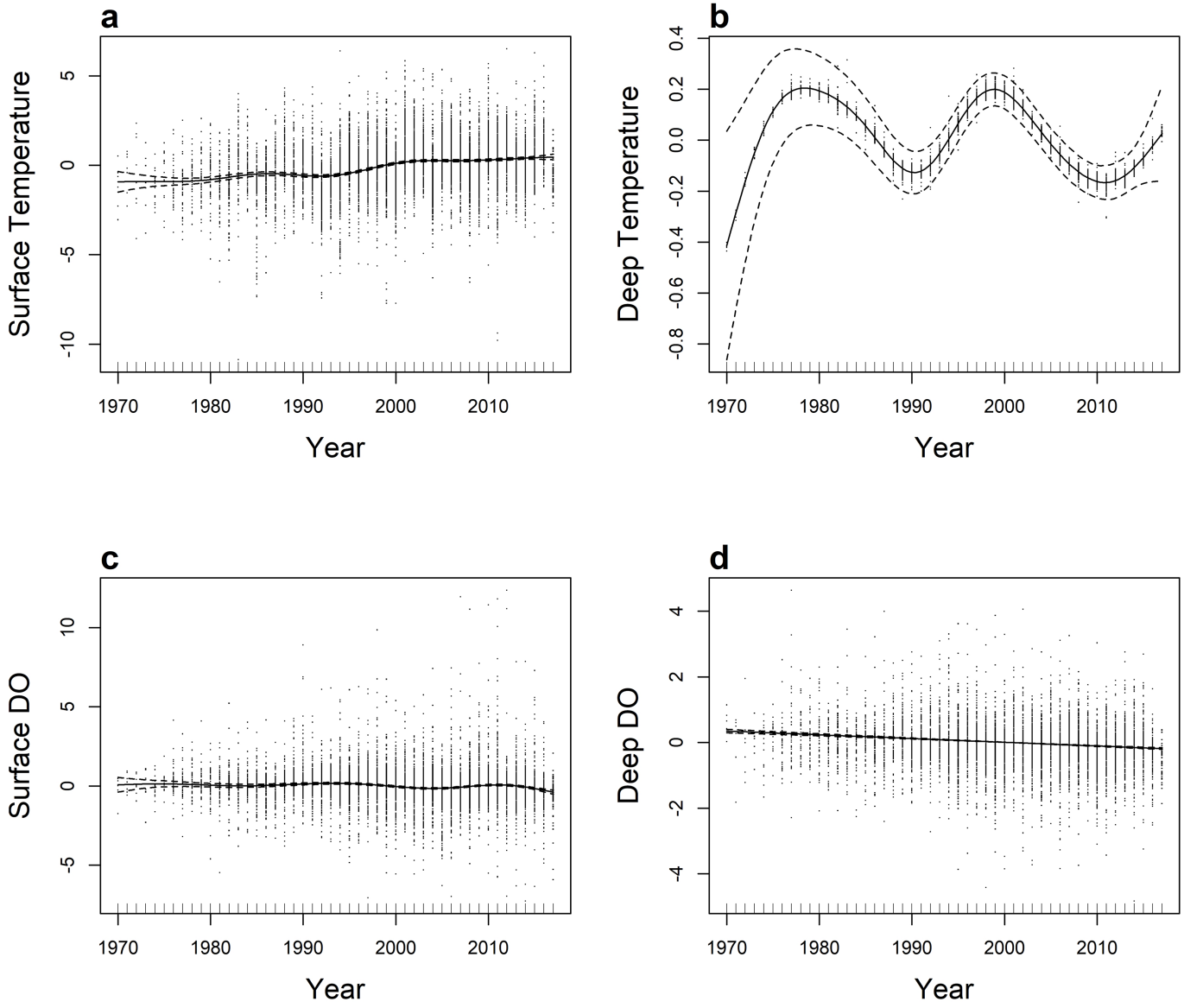

Extended Data Fig. 2 | Results of GAMM analysis of trends zoomed out to visualize distribution of residuals. a, Surface-water temperature (°C). **b**, Deep-water temperature (°C). **c**, Surface-water DO (mg l^{-1}). **d**, Deep-water DO concentration (mg l^{-1}). The error bars are ±1 standard error from the smoothed estimate (as in Fig. 2c–f).

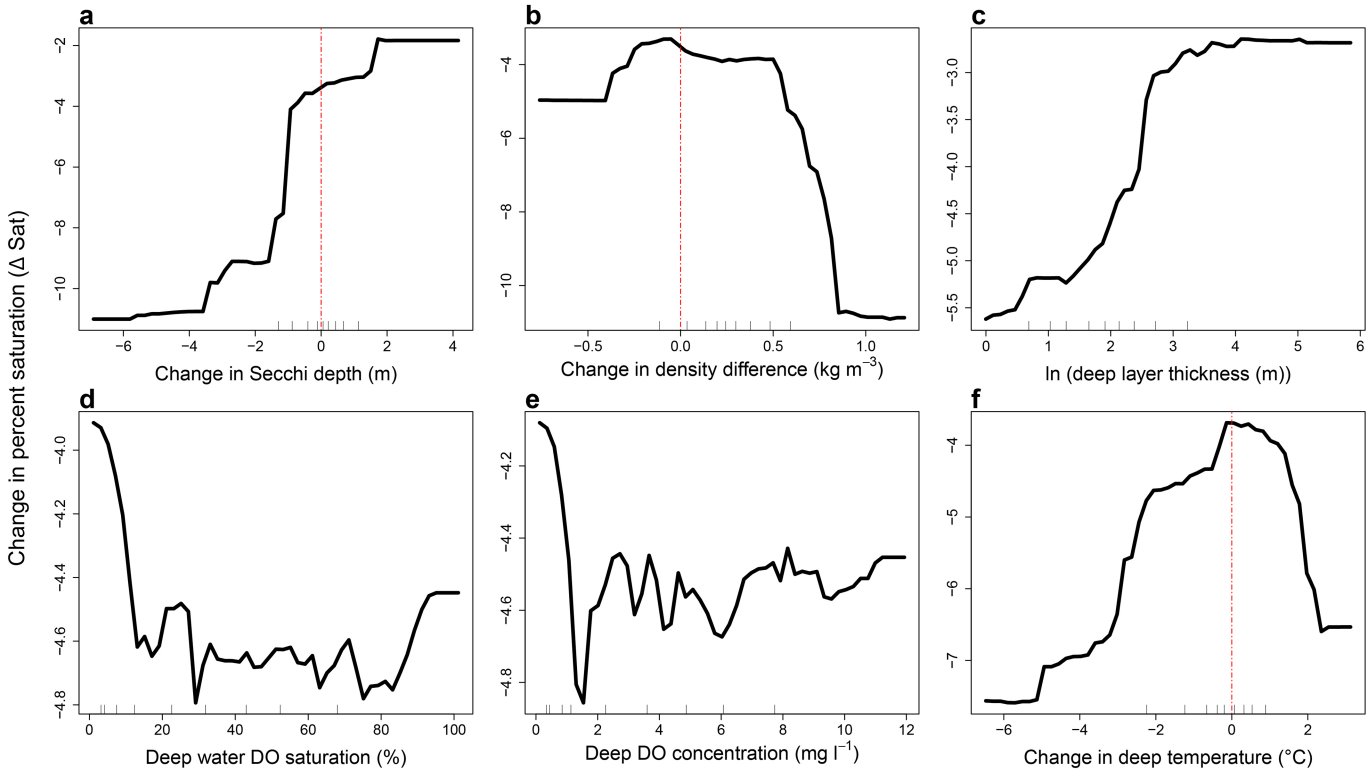

Extended Data Fig. 3 | Drivers of deep-water change in percent dissolved oxygen saturation. a–**f**, Partial dependency plots from a random forest algorithm of deep-water changes in the percentage of dissolved oxygen saturation (ΔSat) in the past five years of record relative to the first five years of record for each lake. Plots are ordered by predictor variable importance, decreasing in importance from the top left to the bottom right. Vertical red lines indicate zero change in predictor variable and hash marks on the *x* axis indicate lake distribution deciles. Partial dependencies indicate the relationship between predictor and response variables when holding other variables at their mean value. Lakes that experienced no change in either water clarity or density difference between surface and deep waters exhibited little change in deep-water saturation (see Fig. 4).

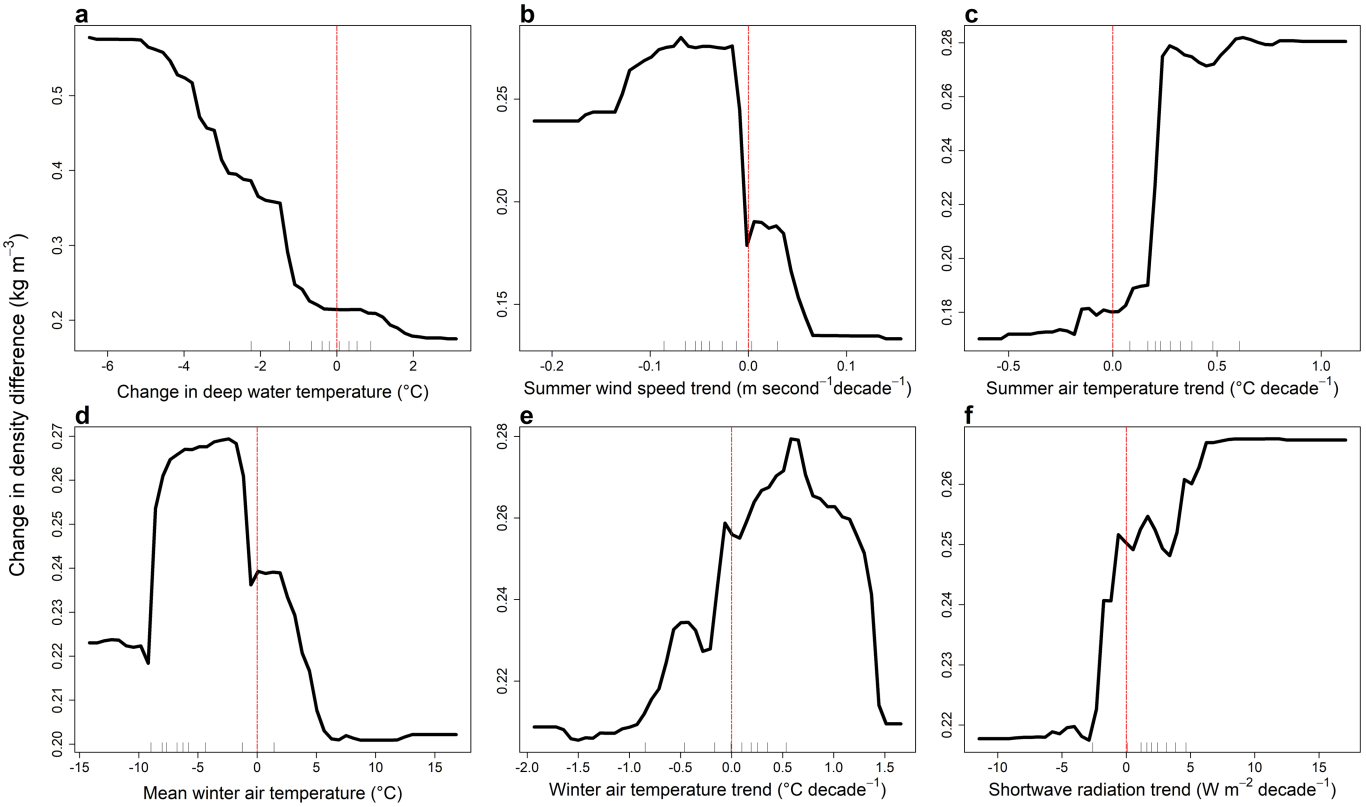

Extended Data Fig. 4 | Drivers of the change in density difference between surface and deep waters. a–f, Partial dependency plots from a random forest algorithm of deep-water change in water column density difference in the last five years of record relative to the first five years of record for each lake. Plots are ordered by predictor variable importance, decreasing in importance from the top left to the bottom right. Vertical red lines indicate zero values for predictor variable and hash marks on the *x* axis indicate lake distribution deciles. Partial dependencies indicate the relationship between predictor and response variables when holding other variables at their mean value.

Extended Data Table 1 | Trends among subsets of temperate lakes, all temperate lakes, and all lakes including eight non-temperate lakes, as well as two time periods: 1980–2017 and 1990–2017

	Trend after subsampling lake rich regions	Trend for all temperate lakes (n=392)	Trend including eight non-temperate lakes (n=400)	1980-2017	1990-2017	Moran's I value	*P* value
Surface water temperature trend (°C decade^{-1})	0.34	0.39	0.38	0.31 (0.12 to 0.51); *P*=0.003	0.34 (0.03 to 0.66); *P*=0.035	0.266	<0.001
Deep water temperature trend (°C decade^{-1})	-0.02	-0.01	-0.02	NS; *P*=0.477	NS; *P*=0.707	0.123	<0.001
Surface water dissolved oxygen (mg l^{-1} decade^{-1})	-0.11	-0.11	-0.11	-0.10 (-0.16 to -0.04); *P*=0.001	-0.17 (-0.28 to -0.05); *P*=0.006	0.18	<0.001
Deep water dissolved oxygen (mg l^{-1} decade^{-1})	-0.16	-0.12	-0.12	-0.12 (-0.20 to -0.05); *P*=0.002	-0.15 (-0.27 to -0.04); *P*=0.012	0.036	0.16
Surface % dissolved oxygen saturation trend						0.174	<0.001
Deep % dissolved oxygen saturation trend						0.017	0.521

Moran's *I* values and associated *P* values describe autocorrelation in select response variables. For temporal subsamples, 95% confidence intervals are included in parentheses.

Extended Data Table 2 | Trends in climate characteristics over study lakes, the entire temperate zone, and temperate zones in selected regions, 1980–2017

Variable (units)	Lake sites	Entire temperate zone	North temperate zone	South temperate zone	Asia	Europe and North America	South America	Southern Africa, Australia, and Oceania
Air temperature (°C decade^{-1})	0.30	0.30	0.33	0.16	0.35	0.31	0.20	0.11
Wind speed (m s^{-1} decade^{-1})	-0.04	0.00	0.00	0.00	0.00	0.00	0.01	-0.01
Summer Precipitation (mm decade^{-1})	-4.23	-0.56	-0.78	0.76	-1.94	0.00	-3.14	3.22
Shortwave radiation (W m^{-2} decade^{-1})	1.88	1.06	1.39	-1.26	1.70	1.04	1.04	-2.14

Extended Data Table 3 | Coefficients and *P* values for the selected multiple regression model predicting lake surface temperature trends

Variable	Coefficient	*P* value	Significance level
Summer air temperature trend	0.1863	0.002	**
Summer wind speed trend	-0.2479	<0.001	***
Summer total precipitation trend	0.0423	0.448	
Summer shortwave radiation trend	0.0386	0.556	
Mean winter temperature	-0.0842	0.199	
Winter air temperature trend	0.0962	0.049	*
Spring air temperature trend	0.1502	0.007	**
Fall air temperature trend	-0.0362	0.464	
Summer wind speed trend * Summer total precipitation trend	0.1681	<0.001	***
Summer total precipitation trend * Spring air temperature trend	0.1718	<0.001	***
Summer total precipitation trend * Fall air temperature trend	0.0872	0.062	.
Summer air temp trend * Summer wind speed trend	-0.1400	0.001	**
Summer wind speed trend * Summer shortwave radiation trend	0.2832	<0.001	***
Summer wind speed trend * Winter air temperature trend	-0.1053	0.004	**
Summer wind speed trend * Mean winter air temperature	0.1469	<0.001	***
Summer wind speed trend * Spring air temperature trend	0.1456	0.006	**
Summer wind speed trend * Fall air temperature trend	0.1215	0.006	**
Summer air temp trend * Spring air temperature trend	-0.0761	0.091	.
Summer shortwave radiation trend * Mean winter air temperature	-0.1725	0.003	**
Summer shortwave radiation trend * Spring air temperature trend	0.1684	0.003	**
Winter air temperature trend * Spring air temperature trend	0.0953	0.057	.
Winter air temperature trend * Fall air temperature trend	0.1074	0.012	*
Mean winter air temperature * Fall air temperature trend	0.1004	0.101	
Spring air temperature trend * Fall air temperature trend	-0.1454	0.002	**

*$P < 0.1$; *$P < 0.05$; **$P < 0.01$; ***$P < 0.001$.